Supplement of Geosci. Model Dev., 14, 7621–7638, 2021
https://doi.org/10.5194/gmd-14-7621-2021-supplement
© Author(s) 2021. CC BY 4.0 License.

Geoscientific Model Development
Open Access
EGU

Supplement of

Reduced-complexity air quality intervention modeling over China: the development of InMAPv1.6.1-China and a comparison with CMAQv5.2

Ruili Wu et al.

Correspondence to: Ruili Wu (wurl15@tsinghua.org.cn, wurl@cnemc.cn)

The copyright of individual parts of the supplement might differ from the article licence.

Table S1 Model configurations in WRFv3.8.

Parameter	Configuration
Simulation Period	Dec. 20, 2016-Dec. 31, 2017
Domain	East Asia (West-to-East:178 × North-to-South:133)
Horizontal resolution	36 km×36 km
Vertical resolution	23 sigma layers from surface to tropopause (100 mb)
Meteorological IC and BC	Reanalysis data from the National Centers for Environmental Prediction Final Analysis (NCEP-FNL)
Shortwave radiation	New Goddard (Chou et al., 1998)
Longwave radiation	RRTM (Mlawer et al., 1997)
Land surface data	USGS
Surface layer	Pleim-Xiu (Xiu and Pleim et al., 2001)
Planetary boundary layer model	ACM2 (Pleim et al., 2007)
Cumulus Parameterization	Kain-Fritsch (Kain et al., 2004)
Cloud microphysics	WSM6
Analysis nudging	Temperature and water vapor mixing (above PBL); Wind (in and above PBL)
Observational nudging	Temperature, water vapor mixing and wind (in and above PBL)
Soil nudging	Include soil moisture and temperature

,

Table S2 Model configurations in CMAQv5.2.

Parameter	Configuration
Simulation Period	Dec. 20, 2016-Dec. 31, 2017
Domain and spatial resolution	East Asia (West-to-East:172 × North-to-South:127) 36 km× 36 km
Vertical resolution	14 sigma levels from surface to tropopause. The values of sigma levels are 1.000, 0.995, 0.988,0.980, 0.970, 0.956, 0.938, 0.893, 0.839, 0.777, 0.702, 0.582, 0.400, 0.200 and 0.000.
IC and BC	GEOS-Chem simulation
Gas-phase mechanism	CB05 gas-phase mechanism with active chlorine chemistry and updated toluene mechanism of (Whitten et al., 2010)
Aqueous-phase mechanism	The updated mechanism of the RADM model (Walcek and Taylor et al., 1986; Chang et al., 1987)
Aerosol module	AERO6
Aerosol thermodynamics	ISORROPIA-II（Fountoukis and Nenes et al., 2007）
Wind blown dust	Not included
The lightening NO_x emissions	Not included
Biogenic emissions	MEGANv2.10 model
Anthropogenic emissions	MEIC inventory for mainland of China emissions in 2017 MIX2010 inventory for the emissions at the region outside the China in East Asia

,

Table S3 WRF evaluation

Variable	Mean_obs	Mean_sim	Sample	Corr	MB	ME	RMSE	NMB (%)	NME (%)
TEMP (°C)	15.03	14.36	502728	0.94	-0.67	2.18	3.07	-6.07	19.95
WSPD (m/s)	2.70	3.04	485075	0.59	0.34	1.48	2.03	12.43	55.39
RH (%)	69.26	73.40	501855	0.79	4.14	9.96	13.28	6.12	14.53

,

Table S4 CMAQ evaluation of 36km spatial resolution across the mainland of China in 2017.

Statistical metrics	$PM_{2.5}$	SO_2	NO_2
Data Pairs	124476	124572	124659
R	0.59	0.39	0.57
Observed Mean (μg/m^3)	45.86	18.52	32.96
Simulated Mean (μg/m^3)	42.12	17.69	28.39
MB (μg/m^3)	-3.74	-0.83	-4.57
RMSE (%)	36.07	25.29	21.91
NMB (%)	-8.16	-4.47	-13.87
NME (%)	50.03	77.15	51.02

,

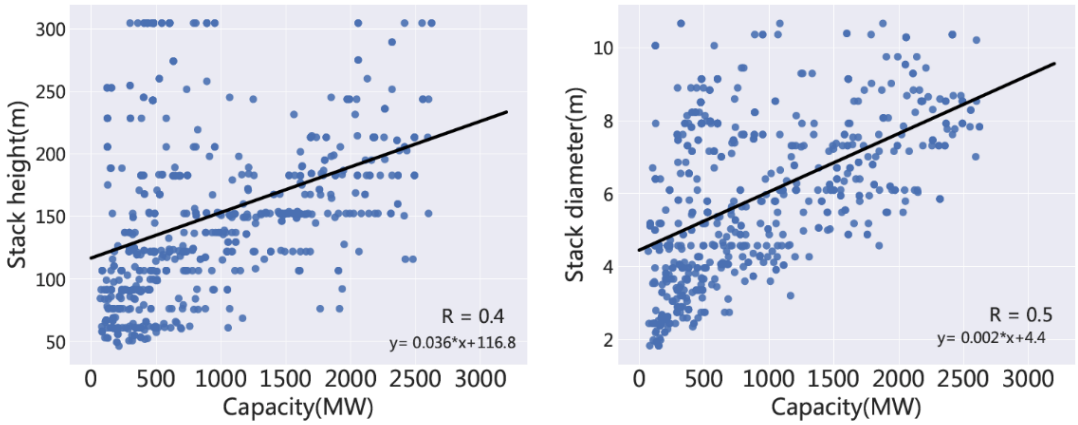

Figure S1 Scatter plot and linear relationship of stack attribution and unit capacity of power plants based on the coal-fired power plant data in 2011 from the national emission inventory in the United States. The stack height and stack diameter are displayed in subplots (a) and (b), respectively.

,

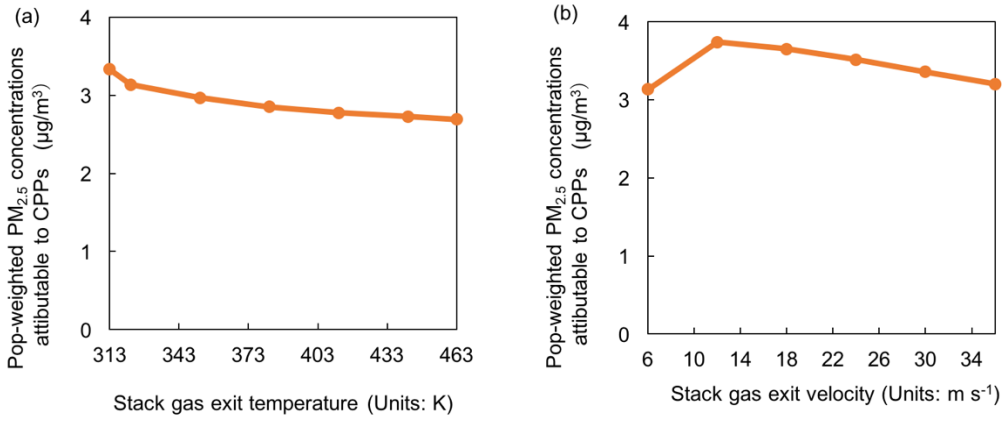

Figure S2 Sensitivity results for two stack attributions of coal-fired power plants. Panel (a) and (b) show the impacts on concentrations of stack gas exit velocity (units: K) and stack gas exit temperature (units: m s^{-1}), respectively.

,

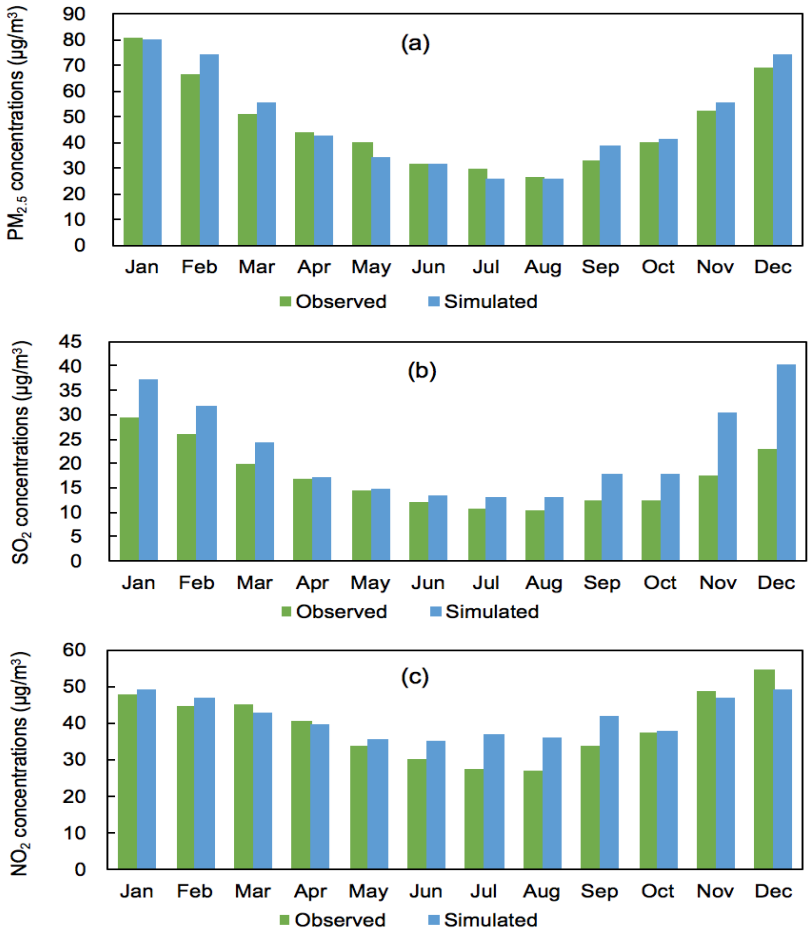

Figure S3 Monthly variations in $PM_{2.5}$, SO_2 ,and NO_2 concentrations simulated by the CMAQ model and comparison with observations.

,

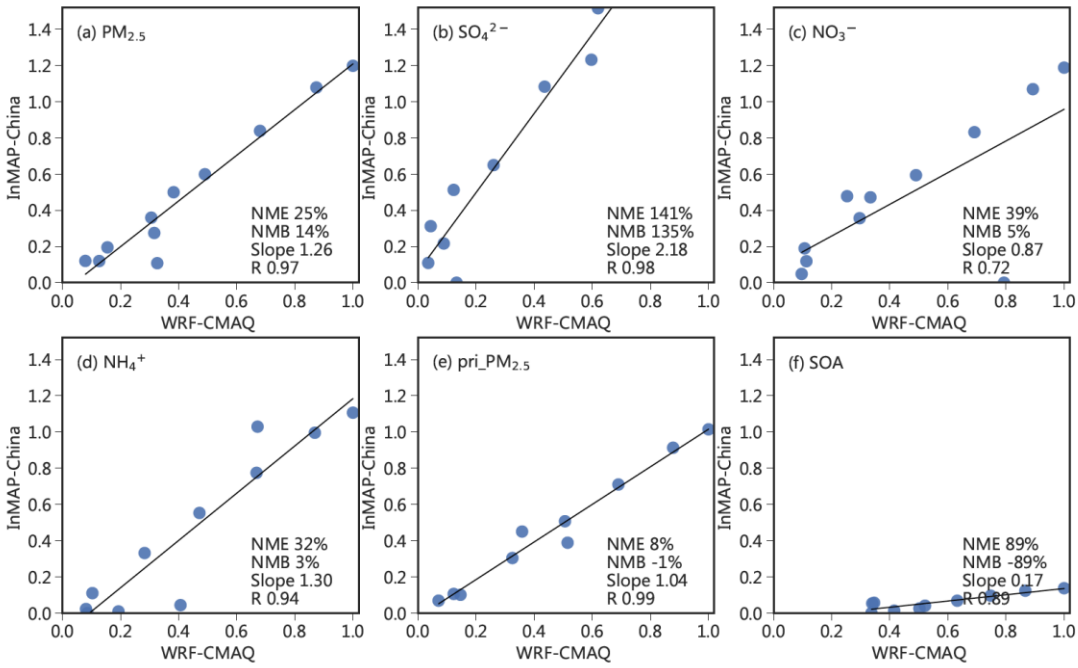

Figure S4 Marginal change in population-weighted $PM_{2.5}$ concentrations and their composition over the BTH region modelled by the InMAP-China and WRF-CMAQ models. The population-weighted pollutant concentration for each scenario is normalized using the largest value among all scenarios modelled by CMAQ. Eleven dots represent the eleven scenarios, and the statistical metrics are labelled in the lower right corner for each panel.

,

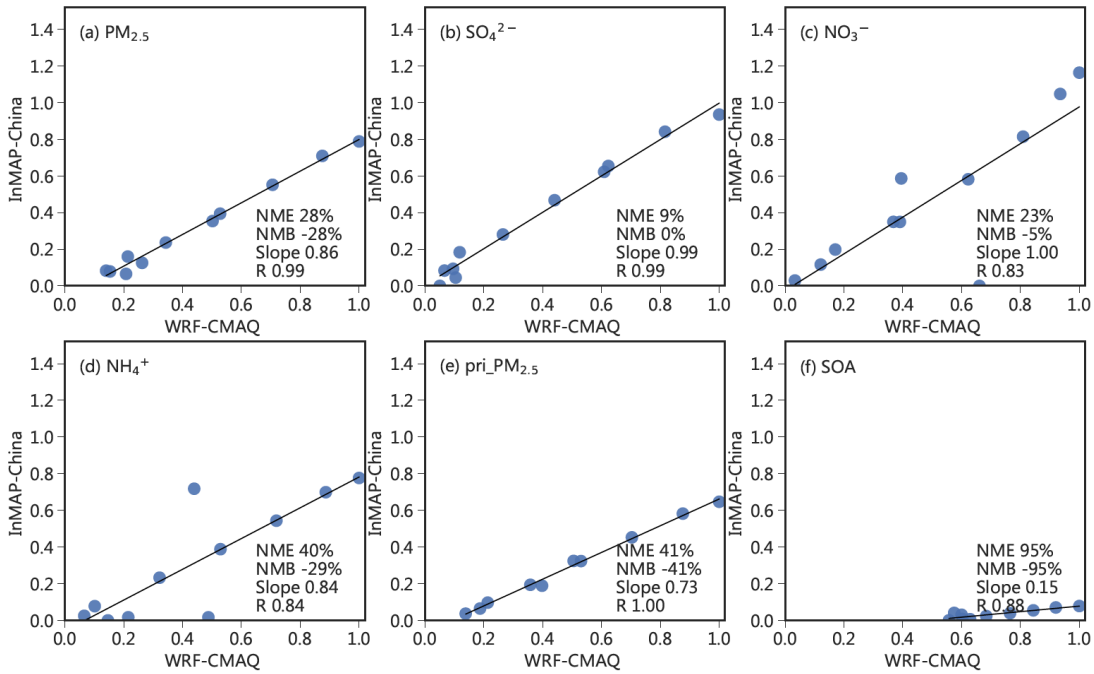

Figure S5 Marginal change in population-weighted $PM_{2.5}$ concentrations and their composition over the PRD region modelled by the InMAP-China and WRF-CMAQ models. The population-weighted pollutant concentration for each scenario is normalized using the largest value among all scenarios modelled by the CMAQ. The eleven dots represent the eleven scenarios, and the statistical metrics are labelled in the lower right corner for each panel.

,

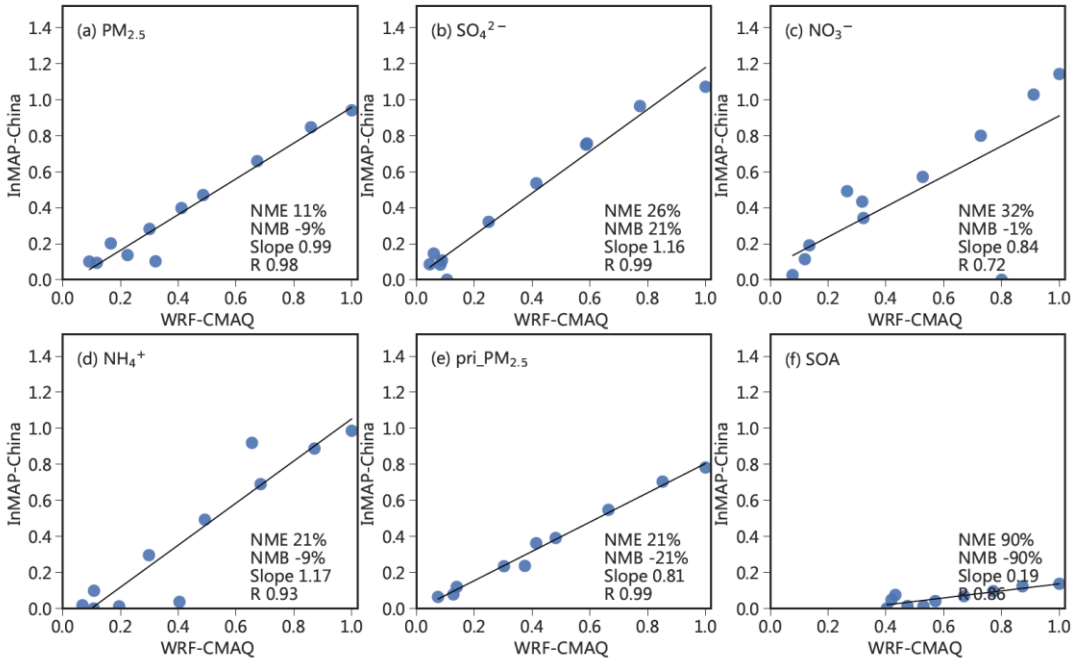

Figure S6 Marginal change in population-weighted $PM_{2.5}$ concentrations and their composition over the YRD region modelled by the InMAP-China and WRF-CMAQ models. The population-weighted air pollutant concentration for each scenario is normalized using the largest value among all scenarios modelled by CMAQ. Eleven dots represent the eleven scenarios, and the statistical metrics are labelled in the lower right corner for each panel.

,

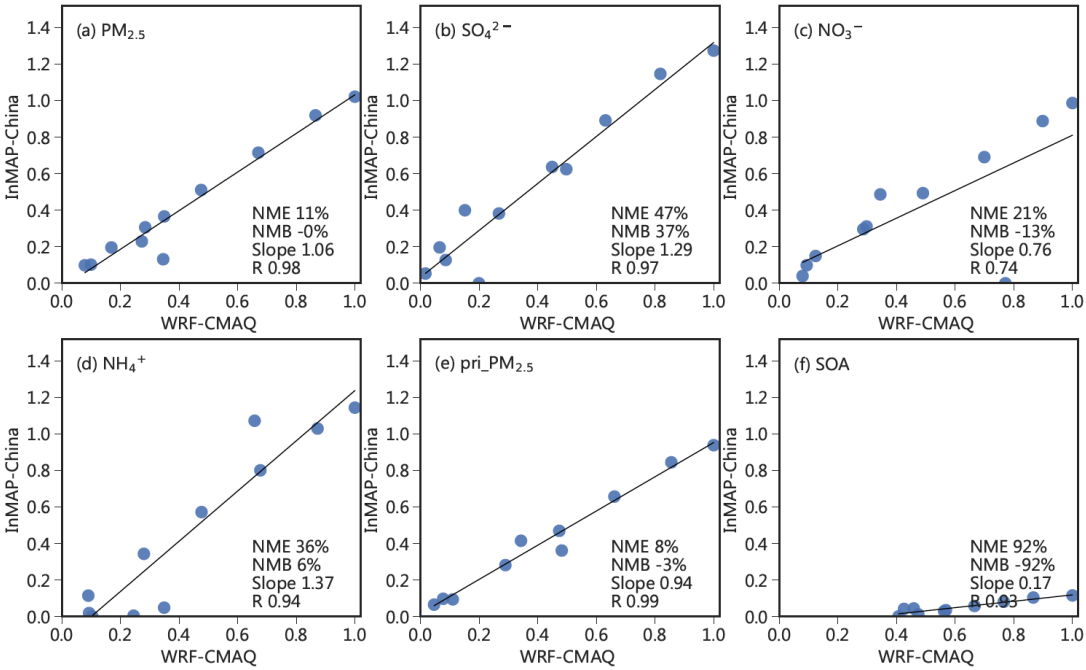

Figure S7 Marginal change in population-weighted $PM_{2.5}$ concentrations and their composition over the Fen Wei Plain region modelled by the InMAP-China and WRF-CMAQ models. The population-weighted air pollutant concentration for each scenario is normalized using the largest value among all scenarios modelled by CMAQ. The eleven dots represent the eleven scenarios, and the statistical metrics are labelled in the lower right corner for each panel.

,

References

Chang,J. S. , Brost, R. A.,Isaksen, I. S. A., Madronich, S., Middleton, P., Stockwell, W. R., Walcek, C. J.:A three-dimensional Eulerian acid deposition model: Physical concepts and formulation. Journal of Geophysical Research, 92:14681-700, https://doi.org/10.1029/JD092iD12p14681,1987.

Chou, M. D., Suarez, M. J., Ho, C. H., Yan, M. M., Lee, K. T.: Parameterizations for Cloud Overlapping and Shortwave Single-Scattering Properties for Use in General Circulation and Cloud Ensemble Models. Journal of Climate, 11(2):202-214, https://doi.org/ 10.1175/1520-0442(1998)0112.0.CO;2, 1998.

Fountoukis, C. and Nenes, A.: ISORROPIA II: A Computationally Efficient Aerosol Thermodynamic Equilibrium Model for K^+, Ca^{2+}, Mg^{2+}, NH_4^+, Na^+, $SO4^{2-}$, NO_3^-, Cl-, H_2O Aerosols, Atmospheric Chemistry Physics, 7, 4639-4659, https://doi.org/10.5194/acpd-7-1893-2007, 2007.

Kain, J. S.: The Kain–Fritsch Convective Parameterization: An Update. Journal of Applied Meteorology. 43:170-81, https://doi.org/10.1175/1520-0450(2004)04360;0170:tkcpau62;2.0.CO;2,2004.

Mlawer, E. J., Taubman, S. J., Brown, P. D., Iacono, M. J., Clough, S. A.: Clough Radiative transfer for inhomogeneous atmospheres: RRTM, a validated correlated-k model for the longwave. Journal of Geophysical Research, 102:16663-82, https://doi.org/10.1029/97jd00237,1997.

Pleim, J. E.: A Combined Local and Nonlocal Closure Model for the Atmospheric Boundary Layer. Part I: Model Description and Testing. Journal of Applied Meteorology and Climatology, 46:1383-95, https://doi.org/10.1175/JAM2539.1, 2007.

Walcek, C. J., Taylor, G.R.: A Theoretical Method for Computing Vertical Distributions of Acidity and Sulfate Production within Cumulus Clouds. Journal of the Atmospheric Science, 43:339-55, https://doi.org/10.1175/1520-0469(1986)0432.0.CO;2,1986.

Whitten, G.Z., Heo, G., Kimura, Y., Mcdonald-Buller, E., Allen, D.T., Carter, W. P. L., Yarwood, G.: A new condensed toluene mechanism for Carbon Bond CB05-TU. Atmospheric Environment, 44(40SI):5346-5355, https://doi.org/10.1016/j.atmosenv.2009.12.029,2010.

Xiu, A., Pleim, J. E.: Development of a Land Surface Model. Part I: Application in a Mesoscale Meteorological Model. Journal of Applied Meteorology, 40:192-209, https://doi.org/10.1175/15200450(2001)040<0192:DOALSM>2.0.CO;2, 2011.

,